Kinematic modelling of tracked vehicles by experimental identification

5 authors, including:

Some of the authors of this publication are also working on these related projects:

Project Tactile Object Recognition View project

Project Spanish project DPI2015-65186-R View project

Kinematic Modelling of Tracked Vehicles by Experimental Identification

J.L. Martínez, A. Mandow, J. Morales, A. García-Cerezo and S. Pedraza

Dpto. Ingeniería de Sistemas y Automática.
Universidad de Málaga
Málaga, Spain
Email: jlmartinez@uma.es

Abstract - **The paper proposes a kinematic approach for tracked vehicles in order to improve motion control and pose estimation. Complex dynamics due to slippage and soil shearing make it difficult to predict the exact motion of the vehicle from the velocity of the two tracks. Nevertheless, reliable geometric approximations are necessary to perform onboard real-time computations for autonomous navigation. The presented solution is based on the kinematic similarities between tracked vehicles and wheeled differential drive vehicles. Particularly, the approximate position of wheel contact points for an equivalent vehicle can be optimized for a particular terrain at moderate speeds. This is achieved off-line by feeding a genetic algorithm with raw trajectory data and reliable localization estimations based on external sensors. The method has been successfully tested for online odometric computations and low-level motion control with the Auriga-α mobile robot. Moreover, the identified parameters are similar to those obtained from the simulated stationary response of a complex dynamic model of this vehicle.**

Keywords - Tracked vehicles; kinematic control; mobile robotics; parameter identification; genetic algorithms.

I. INTRODUCTION

Tracked mobile robots can be useful in applications that demand off-road mobility, such as agricultural, military, forestry, mining and planetary exploration. Locomotion based on tracks offers a large contact area with the ground, which provides better traction than wheels for vehicles on natural terrains [1].

Precisely, the shortcomings of wheels on certain terrains was one of the lessons learned from our experience in agricultural robotics [2], which led to the design and construction of the Auriga-α tracked robot. However, despite obvious control similarities (i.e., differential drive), motion control methods used for differential wheel robots [3] cannot be directly used for tracked vehicles.

Control of tracked vehicles is more complex than in differential drive wheeled vehicles because of the skid steering principle: Variation of the relative velocity of the two tracks results in slippage and soil shearing in order to achieve steering. This means that kinematics is not straightforward, since it is not possible to predict the exact motion of the vehicle only from its control inputs.

Abundant theoretical research on terramechanics has been devoted to the study of mechanics, modelling techniques and track-soil interaction of tracked vehicles [4]. In contrast, we find that little work has been reported on motion control for tracked autonomous mobile robots (which has also been pointed out by other authors interested in this problem [5]). Furthermore, most published works are based on simulated results and use complex vehicle dynamics in some way, which may result too costly for real-time navigation control of an actual robot.

Relevant works devoted to motion control for such vehicles are the following:

- Reference [5] adapted a path-tracking algorithm for wheeled robots by linearizing the force-slip relationship and by feedforward compensation of dynamic friction forces based on simplified models.

- Reference [6] was devoted to real-time estimation of track slippage from inertial readings with an extended Kalman filter. The authors propose that this information could then be used to identify soil model parameters, as well as to eventually adjust motion control.

- Reference [7] addressed the problem of following a planned path at desired speeds by considering lateral friction dynamics in the computation of vehicle's orientation.

The work presented in this paper stemmed from our need to improve motion control and odometric estimations for the Auriga-α robot. The proposed approach is to model kinematics for tracked robots by obtaining an analogy with a wheeled differential drive model. This model can be tuned by means of offline parameter identification from experimental data. Certain simplifying constraints have been considered: planar uniform terrain type, and operation at moderate speeds.

Following this introduction, section 2 discusses kinematic modelling for tracked vehicles based on the instantaneous centers of rotation of the two tracks on the plane. Section 3 describes the estimation of model parameters from experimental data with a genetic algorithm, due to the complex and nonlinear nature of this optimization problem. Section 4 presents experimental results with the Auriga-α mobile robot as well as a comparison with the simulation of a dynamic model. Finally, section 5 offers conclusions and ideas for future work.

II. KINEMATICS FOR TRACKED VEHICLES

Dynamic models of tracked vehicles have proved to be helpful for control design and reliable simulation, but they may result too complex for real-time robot navigation. Alternatively, this section discusses geometric relationships that can be used instead.

The local frame of the vehicle is assumed to have its origin on the center of the area defined by both tracks, and its Y axis is aligned with the forward motion direction. Much in the same way as with differential drive, a tracked vehicle is governed by two control inputs: namely the velocity of its left and right tracks (V_l, V_r). Then, direct kinematics could be stated as follows:

$$(v_x, v_y, \omega_z) = f_d(V_l, V_r) \tag{1}$$

where (v_x, v_y) is the vehicle's linear velocity with respect to its local frame, and ω_z is its angular velocity. Conversely, finding control actions that result in a desired motion can be expressed as the inverse kinematics problem:

$$(V_l, V_r) = f_i(v_x, v_y, \omega_z) \tag{2}$$

For planar motion, the *Instantaneous Center of Rotation* (ICR) of a vehicle, considered as a rigid body, is defined as the point in the plane where the motion of the vehicle can be represented by a rotation and no translation occurs.

In the planar motion of a tracked vehicle, not only the motion of the entire vehicle can be taken into account, but also the motion of each of its tracks on their contact surface with the ground. The angular velocity of the two tracks on the plane is the same as that of the vehicle, since they cannot rotate around the vehicle's Z axis.

A track can be modelled as a rigid body with an extra degree of freedom, which is the rolling speed of the track. Thus, the motion of the points of a track is the composition of the motion of the vehicle and that of track rolling. Because of this, the ICR of a track on the plane is different from the ICR of the entire vehicle (see Fig. 1).

In fact, the ICRs of tracks on the plane lie on *a priori* unknown positions of a line parallel to the local X axis, which also contains the ICR of the entire vehicle, because of Kennedy's ICR theorem [8]. Note that the above discussion refers to the ICR of tracks on the ground plane, not to their roll axis.

Coordinates on the local frame for the ICR of the entire vehicle (ICR) and for the ICRs of its left and right tracks (ICR$_l$ and ICR$_r$, respectively) can be geometrically obtained as:

$$x_{ICR} = \frac{-v_y}{\omega_z} \tag{3}$$

$$y_{ICR} = y_{ICR_l} = y_{ICR_r} = \frac{v_x}{\omega_z} \tag{4}$$

$$x_{ICR_l} = \frac{V_l - v_y}{\omega_z} \tag{5}$$

$$x_{ICR_r} = \frac{V_r - v_y}{\omega_z} \tag{6}$$

where $v=(v_x,v_y)$ is the translational velocity of the vehicle in local coordinates. It must be noted that the x coordinate of the ICR for the entire vehicle ranges from $\pm\infty$ depending on its curvature, whereas track ICR coordinates x_{ICRl} and x_{ICRr} are bounded for a given velocity range [9].

If the inverse functions are computed, instantaneous translational and rotational speeds with respect to the local frame can be obtained as:

$$v_x = \frac{V_r - V_l}{x_{ICR_r} - x_{ICR_l}} \, y_{ICR} \tag{7}$$

$$v_y = \frac{V_r + V_l}{2} - \frac{V_r - V_l}{x_{ICR_r} - x_{ICR_l}} \frac{x_{ICR_r} + x_{ICR_l}}{2} \tag{8}$$

$$\omega_z = \frac{V_r - V_l}{x_{ICR_r} - x_{ICR_l}} \tag{9}$$

These equations represent the direct kinematics of the vehicle as stated by (1) if the ICRs of the left and right tracks can be properly estimated.

On the other hand, inverse kinematic relations can be expressed by:
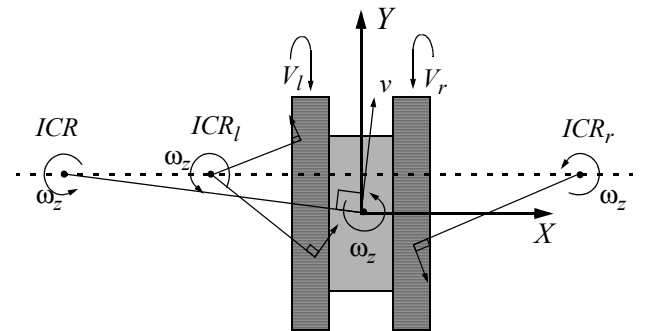

Figure 1. Instantaneous centers of rotation on the plane. The entire vehicle as a rigid body follows a circular course about ICR, which lies on the axis defined by ICR$_l$ and ICR$_r$.

$$V_l = \sqrt{\|v\|^2 - y_{ICR}^2 \omega_z^2} + x_{ICR_l} \, \omega_z \qquad (10)$$

$$V_r = \sqrt{\|v\|^2 - y_{ICR}^2 \omega_z^2} + x_{ICR_r} \, \omega_z \qquad (11)$$

which includes a non-holonomic restriction, since v_x and v_y references cannot be imposed separately.

It must be noted that these same expressions also represent direct and inverse kinematics for wheeled differential drive vehicles. Then, for instantaneous motion, kinematics for both types of vehicle are equivalent, as illustrated in Fig. 2.

The difference between the two traction schemes is that whereas ICRs for ideal wheels without lateral sliding are constant and lie on the ground contact points, track ICRs are dynamics-dependent and always lie outside of the tracks because of slippage. Thus, less slippage means that the ICRs are closer to the vehicle.

Moreover, the position of the center of mass of the vehicle significantly affects track ICRs. The closer the center of mass is to one side, the lesser that side's track will slip on account of pressure, and the closer its ICR will be. Furthermore, less slippage occurs if the center of mass is closer to the front or rear end of the vehicle, since pressure distribution is concentrated onto a portion of the track contact surface. This results in closer track ICRs.

A steering efficiency index of the vehicle can be defined as the normalized distance between the track ICRs:

$$c = \frac{x_{ICR_r} - x_{ICR_l}}{L}; \quad (c \geq 1) \qquad (12)$$

where L is the distance between track centerlines. Index c is equal to 1 when no slippage occurs (i.e., ideal differential drive vehicles).
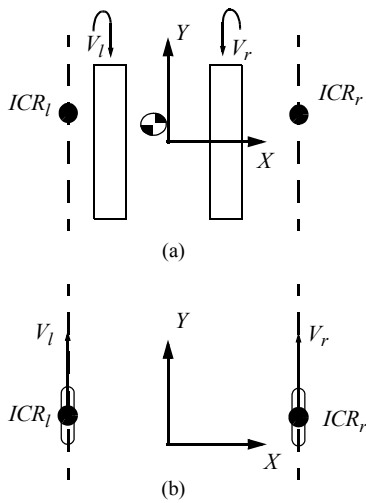

(a)

(b)

Figure 2. Equivalence of tracked (a) and differential drive (b) kinematics for instantaneous motion.

Similarly, a normalized eccentricity index can be defined as follows:

$$e = \frac{x_{ICR_r} + x_{ICR_l}}{x_{ICR_r} - x_{ICR_l}} \qquad (13)$$

Index e is equal to 0 when track ICRs are placed symmetrical with respect to the local Y axis.

The major consequence of the discussion above, is that the effect of vehicle dynamics is introduced in the kinematic model just by two points in local coordinates: ICR_l and ICR_r.

III. IDENTIFICATION OF TRACK ICRs WITH A GENETIC ALGORITHM

This section describes how the analogies presented in section II have been considered to approximate a dynamics-free tracked kinematic model. This means identifying optimized constant values of track ICRs for a given set of working conditions. Optimization is required since actual track ICR positions vary during navigation on account of dynamics.

Thus, the identification problem consists on finding three parameters:

- The local Y coordinate of track ICRs ($y_{ICR_l} = y_{ICR_r} = y_{ICR}$).

- The local X coordinates of both track ICRs (x_{ICR_r} and x_{ICR_l}).

Parameter identification consists of two steps. The first one is to obtain experimental data. Then, an optimization tool is employed to find the parameter values that best fit the data.

Genetic Algorithms (GAs) are proposed in this case. This is a derivative-free stochastic optimization tool, where each point in a solution space is encoded into a bit string (chromosome) and is associated with a fitness value. Starting from an initial random population, points with better fitness values are used to construct a new population of solutions by means of genetic operators. Thus, after several iterations (generations), the overall fitness value is improved [10].

GAs are useful for finding optimized track ICR parameters ($x_{ICR_l}, x_{ICR_r}, y_{ICR}$) from experimental data because no significant *a priori* knowledge exists about them, they can be easily coded as bit strings, and a way can be devised to assign a fitness value to new solutions.

In the first place, a number of training paths are followed by the mobile robot, where it is subject to diverse rotational and translational speeds and accelerations. Both internal and external sensor data are recorded during these experiments. These paths are then divided into N independent short segments, in such a way that the pose of the vehicle can be

accurately determined at both ends of each segment from external readings. The minimum length of the segment is determined by the external sensor rate. Every segment must comprise several odometric samples (e.g. shaft encoder data or inertial measurement). Then, parameter identification can be performed offline.

Fitness of the alternative solutions evaluated by the GA can be assessed by computing the sum of the squared odometric errors for the N training segments:

$$J(x_{ICR_l}, x_{ICR_r}, y_{ICR}) =$$
$$\sum_{i=1}^{N} \left((\Delta x_i - \Delta \hat{x}_i)^2 + (\Delta y_i - \Delta \hat{y}_i)^2 + (\Delta \phi_i - \Delta \hat{\phi}_i)^2 \right) \quad (14)$$

where $(\Delta \hat{x}_i, \Delta \hat{y}_i, \Delta \hat{\phi}_i)$ is the estimated pose increment of the vehicle obtained by integrating (7)-(9) along the i-th segment. The triplet $(\Delta x_i, \Delta y_i, \Delta \phi_i)$ stands for the actual localization of the vehicle relative to the origin of each segment, which has to be computed by means of a precise localization method based on external sensors (e.g., laser range-finder or ultrasonic transducers).

Thus, at each GA iteration, the solutions with minimum overall error are chosen for computing a new population with the crossover and mutation operators.

As a result of this method, constant ICR parameters $(x_{ICR_l}, x_{ICR_r}, y_{ICR})$ could be optimized for a specific robotic task, according to typical path motions, particular soil types, and speed ranges. These values can then be applied online for motion estimation and control.

IV. EXPERIMENTAL RESULTS

A. Auriga-α Mobile Robot

The method presented in the paper has been applied to the Auriga-α mobile robot (see Fig. 3). Its dimensions are 1.24m(l)x0.75m(w)x0.84m(h), and weights approximately 258Kg. This vehicle is powered by an on-board petrol-fed AC generator, although a power cable socket is also available for indoor tests.

Locomotion is based on two independent DC motors fitted with 1:38 gear-reductions and incremental shaft encoders for dead-reckoning. Each track contains 4 rollers as well as sprockets at both ends, of which the foremost one is linked to the output gear shaft. The rubber belts are 0.15m wide, with a longitudinal contact surface of 0.7m and $L=$ 0.42m. The top speed of each track is 1m/s.

Two control systems can be distinguished in the mobile robot Auriga-α:

- The DSP-based motor control interface, which accepts track speed setpoints from either the manual control joystick or the navigation controller and also

provides actual track speeds.

- The navigation system, which includes the low-level controller and the path tracker. An industrial PC based on a Pentium-IV microprocessor at 2.2GHz governs navigation under a real-time operating system every T= 25ms.

The on-board laser device employed for self-localization is a conventional time-of-flight range scanner (LMS-200), which scans a plane parallel to the ground at a height of 0.55m in front of the vehicle. It has the following features: 180° field-of-view, 0.5° angular resolution, exploration range of up to 50m, and range errors of ±1 cm. Every 0.25s, a new scan is transmitted to the navigation PC through the serial port, using the RS-232 protocol at 38400 bauds.

B. Identification Experiments

In our earliest control efforts with Auriga-α, a simple differential drive model, which considered that the tracks were equivalent to wheels rolling on the local X axis (i.e., efficiency $c=1$ and eccentricity $e=0$) was used. It soon became clear that this model did not work well, so it was enhanced by supposing symmetric track ICRs, i.e. $e=0$ and $y_{ICR}=0$. Parameter c was experimentally estimated by issuing equal opposite track speeds, which results in an approximately pure rotation of the vehicle about its Z axis.

Then, the following equation was applied:

$$c = \frac{\int V_r \, dt - \int V_l \, dt}{L \, \phi} \quad (15)$$

where ϕ represents the rotated angle. The average result after several tests was c=1.90 [11].

The method described in the paper allows for a more realistic asymmetric model. What follows is a description of

Figure 3. The Auriga-α mobile robot.

the implementation details of section III. First, experimental data were collected from encoder readings as well as an onboard laser scanner in combination with a reliable localization procedure that matches consecutive scans [12]. The laser scan rate allows accurate localization of the vehicle as much as every 0.25s. Between scans, 10 sets of internal readings are available for odometric estimation. These 0.25s intervals, recorded during a robot path, are used as the short segments in the GA identification procedure discussed in section III.

The training experiments resulted in N=1807 segments, obtained from 9 different manually guided paths (about 20m long each) over a flat hard-surface soil. The GA method has been applied independently to each of the 9 paths, resulting in the identified parameters shown in Table I. As expected, the optimized parameters are dependent of the training path. Nevertheless, it must be noted that the standard deviation σ does not exceed 1.8cm for any parameter. This table also shows the mean values computed from all paths weighed according to the partial number of segments. These results imply that the center of mass of the vehicle lies not on its geometric center, but is closer to its left side and slightly forward. The steering efficiency and eccentricity indexes are c=1.847 and e=0.083 respectively.

C. Odometric Estimation

A validation path, different from those used for training the GA, has been used to test odometric estimation with Auriga-α. This path is depicted in Fig. 4 as a dotted line. Surrounding walls and environment obstacles are shown in the figure as a result of overlapping points from N=174 consecutive laser scans [12]. For simplicity, it has been assumed that the world frame is fixed at the starting localization of the path.

TABLE I
GA RESULTS FOR THE TRAINING EXPERIMENTS

#	N	y_{ICR}	x_{ICRl}	x_{ICRr}
1	139	0.0605	-0.3823	0.4246
2	158	0.0317	-0.3469	0.4286
3	234	0.0373	-0.3616	0.4273
4	199	0.0193	-0.3495	0.4027
5	206	0.0363	-0.3711	0.4192
6	143	0.0528	-0.3640	0.3989
7	159	0.0453	-0.3571	0.4378
8	346	0.0147	-0.3391	0.4201
9	223	0.0388	-0.3510	0.4220
M		**0.0343**	**-0.3558**	**0.4202**
σ		0.0177	0.0117	0.0151

TABLE II
SEGMENT PERFORMANCE ON VALIDATION PATH

$*10^3$	$\Sigma e_x^2/N$	$\Sigma e_y^2/N$	$\Sigma e_\phi^2/N$	J/N
Asymmetric	0.0327	0.0541	0.0334	0.1202
Symmetric	0.0376	0.0618	0.0615	0.1609

The performance of our earlier symmetric model with c=1.9 is shown as a dashed line in Fig. 4. It is clearly seen that although the length and the overall shape of the path are estimated, accumulated errors (mainly in heading) result in an important pose deviation at the end of the path.

The solid line in Fig. 4 shows the estimated path according to the kinematic model defined by the identified parameters x_{ICRl}=-0.3558m, x_{ICRr}=0.4202m, and y_{ICR}=0.0343m. Even if there is still a small deviation both in heading and position (as expected for odometry) the result offers a quite accurate estimation of the original path, and clearly improves the symmetric approach.

Performance of both models regarding individual segments is summarized in Table II. This table shows the mean value of the squared pose error (J) as well as the squared x, y and ϕ errors for the N=174 segments of the validation path. Interestingly, the heading component has been mostly improved. This short-term performance of the kinematic model is useful for the low-level control of the vehicle in order to transform linear and angular velocity setpoints for the vehicle into appropriate track speeds.

D. Dynamic Modelling

An analytical study of the stationary response for the same vehicle and terrain type involving dynamics and computer simulation [9] is also useful for validating the proposed experimental method. Since motor drives with large reduction act as low pass filters, stationary response of the dynamic system provides a good approximation of its behavior.

Basically, the model consists of force and moment equations dependent on soil mechanics and vehicle dynamics. Track-soil interaction is modelled by the pressure and friction fields. A bidimensional distribution of pressures along the contact area of each track has been considered. This distribution is linear in the longitudinal axis and
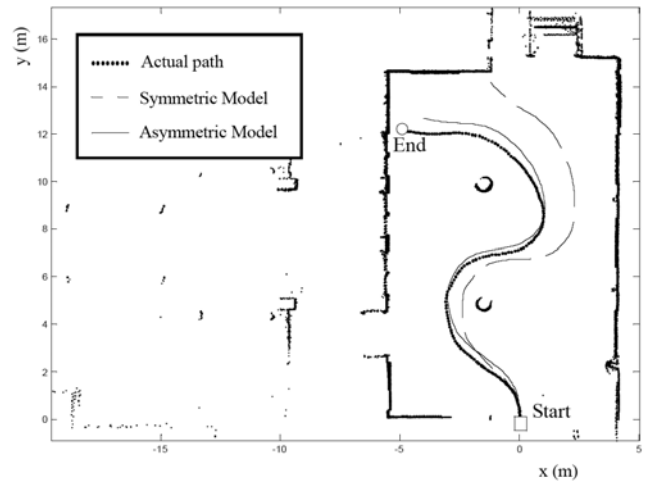

Figure 4. Odometric estimations against the actual path over a laser-based map.

transversely constant. For friction, a Coulomb law has been considered which is valid for hard surface soils.

From the analysis of mass distribution within the vehicle, the position of the center of mass has been estimated in local coordinates as (-0.015m, 0.04m). Fig. 5 shows clouds of track ICRs obtained by combining equidistant track speeds along the (-1m/s,+1m/s) interval. It has been observed that less dispersion in ICR_l points than in ICR_r points is due to the position of the center of mass. This agrees with the standard deviation values in Table I.

The estimated constant coordinates for track ICRs that better fit the overall stationary response of the dynamic model are the following: x_{ICRl}= -0.375m, x_{ICRr}=0.457m, and y_{ICR}=0.0492m. The efficiency and eccentricity indexes are c=2.011 and e=0.098 respectively. These results are consistent with the ones obtained with the experimental method proposed in the paper.

V. CONCLUSIONS

The work presented in this paper originates from the need to control the motion of a tracked autonomous mobile robot. The aim was to improve real-time navigation without introducing complex dynamics in the loop.

We have established a kinematic similarity between tracked and wheeled traction based on the ICRs of the tracks on the plane. This allows that conventional path tracking methods can be employed without modifications.

Track ICR positions are not constant during navigation, but they are bounded within an area in the vicinity of the vehicle for a given velocity range. Then, optimized values for a specific robotic task, according to typical path motions, particular soil types, and speed ranges have been obtained by means of a GA with actual sensor data from several paths.

Moreover, a theoretical dynamic analysis of the vehicle, in which track ICRs have been computed for the whole

working range of track speeds, has also been performed. Its results confirm the optimized experimental model.

The motion control accuracy (i.e., pose estimation given a history of odometric readings, and computation of control inputs so that the robot can obtain desired motion) with the Auriga-α mobile robot has been drastically improved with respect to previous kinematic models.

Even if results have been favorable for a case that represents many autonomous robot applications, it would be interesting to test the proposed approach with other types of tracked vehicles (i.e., heavier and faster) and terrains.

REFERENCES

[1] M.G. Bekker (1956) *Theory of Land Locomotion*. The University of Michigan Press, Ann Arbor.

[2] A. Mandow, J. Gómez-de-Gabriel, J.L. Martínez, V.F. Muñoz, A. Ollero, A. García-Cerezo (1996) "The Autonomous Greenhouse Operation Mobile Robot Aurora." *IEEE R&A Magazine* R&A Society, pp. 18-28.

[3] A. Ollero, A. García-Cerezo, J.L. Martínez and A. Mandow (1997) "Fuzzy Tracking Methods for Mobile Robots." *Applications of Fuzzy Logic: Towards High Machine Intelligence Quotient Systems*, Vol. 9, Chap. 17, pp. 347-364, Prentice Hall Series on Environmental and Intelligent Manufacturing Systems.

[4] J.Y. Wong (1993) *Theory of Ground Vehicles*. 2nd Edition. Wiley, New York.

[5] M. Ahmadi, V. Polotski and R. Hurtea (2000) "Path Tracking Control of Tracked Vehicles." *Proc. of the IEEE Int. Conf. on Robotics & Automation*, San Francisco, CA.

[6] A.T. Le, Rye, and Durrant-Whyte H.F. (1997) "Estimation of Track-soil Interactions for Autonomous Tracked Vehicles." *Proc. of the 1997 IEEE Int. Conf. on Robotics and Automation, Albuquerque, New Mexico.*

[7] Z. Shiller, D.C. Serate and M. Hua (1993) "Trajectory Planning of Tracked Vehicles". *Proc. of the IEEE Int. Conf. on Robotics and Automation*, vol. 3, pp. 796-801.

[8] J.E. Shigley and J.J. Uiker (1980) *Theory of Machines and Mechanisms. McGraw Hill Text.*

[9] S. Pedraza (2000) *Modelado y Análisis de Vehículos de Cadenas para la Navegación Autónoma* (in Spanish). Ph D. Thesis, Universidad de Málaga, Spain.

[10] D.E. Goldberg (1989) *Genetic Algorithms in Search, Optimization, and Machine Learning.* Addison-Wesley, Reading, MA.

[11] S. Pedraza, R. Fernández, V.F. Muñoz and A. García-Cerezo (2000) "A motion control approach for a tracked mobile robot." *Proc. of the 4th IFAC Int. Symposium on Intelligent Components and Instruments for Control Applications*, pp. 147-151, Buenos Aires, Argentina

[12] J.L. Martínez (2003) "Mobile Robot Self-Localization by Matching Successive Laser Scans via Genetic Algorithms." *Proc. of the 5th IFAC International Symposium on Intelligent Components and Instruments for Control Applications*. Aveiro, Portugal.
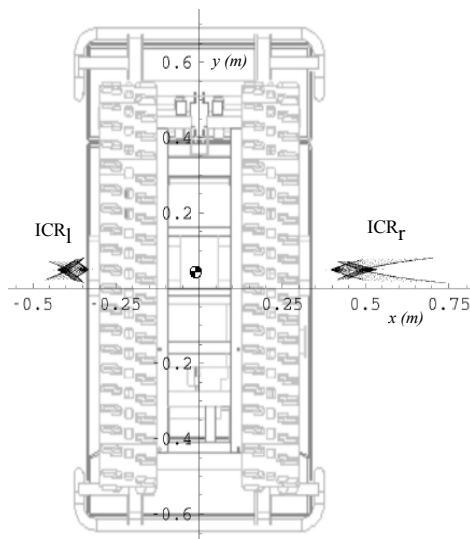
Figure 5. Dynamic analysis of track ICRs for the Auriga-α mobile robot.